

See discussions, stats, and author profiles for this publication at: <https://www.researchgate.net/publication/332951428>

# Joint Optimization of UAV Position, Time Slot Allocation, and Computation Task Partition in Multiuser Aerial Mobile-Edge Computing Systems

Article in IEEE Transactions on Vehicular Technology · May 2019

DOI: 10.1109/TVT.2019.2915836

CITATION

1

READS

86

5 authors, including:



Miao Jiang

Sun Yat-Sen University

12 PUBLICATIONS 97 CITATIONS

SEE PROFILE



Qi Zhang

Sun Yat-Sen University

90 PUBLICATIONS 1,184 CITATIONS

SEE PROFILE



Quanzhong Li

Sun Yat-Sen University

75 PUBLICATIONS 1,070 CITATIONS

SEE PROFILE

# Joint Optimization of UAV Position, Time Slot Allocation, and Computation Task Partition in Multiuser Aerial Mobile-Edge Computing Systems

Jiawen Hu, Miao Jiang, Qi Zhang, *Member, IEEE*, Quanzhong Li, and Jiayin Qin

**Abstract**—In this paper, an unmanned aerial vehicle (UAV)-enabled mobile edge computing (MEC) server is considered to provide MEC services for multiple ground users by employing a time-division multiple access protocol. Our objective is to solve the joint optimization problem of UAV position, time slot allocation, and computation task partition, which minimizes the system energy consumption of all users while ensuring the successful task computation of all users during a time block. We propose a globally optimal solution which is found by two-dimensional search over possible UAV positions. In each search, we theoretically derive the semi-closed-form solution to the joint optimization of time slot allocation and computation task partition by employing augmented Lagrangian active set method. An alternating optimization scheme to find the locally optimal solution is also proposed. It is shown through numerical results that our proposed schemes are superior to the no offloading, full offloading, and gravity center offloading schemes.

**Index Terms**—Augmented Lagrangian active set, mobile edge computing (MEC), unmanned aerial vehicle (UAV).

## I. INTRODUCTION

Mobile edge computing (MEC) is a promising technology to provide improved computing capability for energy-constrained wireless devices [1]–[7]. In [2], the dynamic offloading for MEC systems was proposed by using Lyapunov optimization. In [3] and [5], the joint computation and communication resource allocation schemes in single-user and multiuser MEC systems were investigated, respectively.

The aforementioned works do not consider that the MEC server is mounted on an unmanned aerial vehicle (UAV) [8]–[16]. Conventionally, UAVs are employed to provide reliable wireless communications to ground users [8]–[16]. In disaster response, emergency relief or military scenarios, the use of

UAV-enabled MEC server plays an important role in the execution of data analytics application for the assessment of the status of victims, enemies, or hazardous terrain and structures [17]. In [17], [18], joint offloading optimization and trajectory design for aerial MEC systems was studied. However, to our best knowledge, the research on joint optimization of UAV position, time slot allocation, and computation task partition in multiuser aerial MEC systems is still missing.

In this paper, we consider that a UAV integrated with an MEC server provides MEC services for multiple ground users by employing a time-division multiple access (TDMA) protocol. Our goal is to minimize the system energy consumption of all users while ensuring the successful task computation of all users during a time block. We theoretically derive a globally optimal solution to the optimization problem. The globally optimal solution is found by two-dimensional (2D) search over possible UAV positions, where in each iteration, the semi-closed-form solution to the joint optimization of time slot allocation and computation task partition is found by augmented Lagrangian active set method. To reduce the computational complexity, we also propose an alternating optimization scheme to find the locally optimal solution to the optimization problem.

The differences between our work and those in [17], [18] are detailed as follows. The former considers delay-sensitive scenarios where the UAV-enabled MEC server should serve multiple users simultaneously whereas the latter consider delay-insensitive scenarios where the MEC server serves multiple users sequentially. Therefore, the former focuses on the UAV position optimization problem whereas the latter focus on the UAV trajectory optimization problem. Furthermore, the former obtains both the globally and locally optimal solutions to the joint optimization problem whereas the latter only obtain the locally optimal solution.

## II. SYSTEM MODEL AND PROBLEM FORMULATION

A UAV integrated with an MEC server is considered in this paper, which serves  $K$  users on the ground. We assume that the UAV is flying at a fixed altitude  $H > 0$  above the ground. The three-dimensional (3D) coordinate of the UAV is denoted as  $\mathbf{w}_0 = (x_0, y_0, H)^T$ . The 3D coordinate of user  $k$ ,  $k \in \mathcal{K} = \{1, 2, \dots, K\}$  is denoted as  $\mathbf{w}_k = (x_k, y_k, 0)^T$ . The 3D coordinates of all users are known in advance at the UAV for its position design and resource allocation [8], [10], [15]. The line-of-sight (LOS) paths between the UAV and all

Copyright (c) 2015 IEEE. Personal use of this material is permitted. However, permission to use this material for any other purposes must be obtained from the IEEE by sending a request to pubs-permissions@ieee.org.

This work was supported in part by the National Natural Science Foundation of China under Grant 61672549 and Grant 61802447, in part by the Guangdong Natural Science Foundation under Grant 2018B0303110016, and in part by the Guangzhou Science and Technology Program under Grant 201607010098 and Grant 201804010445.

J. Hu, M. Jiang, Q. Zhang, and J. Qin are with the School of Electronics and Information Technology, Sun Yat-sen University, Guangzhou 510006, Guangdong, China, and also with the Key Laboratory of Machine Intelligence and Advanced Computing (Sun Yat-sen University), Ministry of Education, China (e-mail: hujw25@mail2.sysu.edu.cn, jmiao@mail2.sysu.edu.cn, zhqi26@mail.sysu.edu.cn, issqjy@mail.sysu.edu.cn). Q. Li is with the School of Data and Computer Science, Sun Yat-sen University, Guangzhou 510006, Guangdong, China (e-mail: liquanzh@mail.sysu.edu.cn). J. Qin is also with Xinhua College of Sun Yat-sen University, Guangzhou 510520, Guangdong, China.

users on the ground are assumed to exist because the UAV is flying relatively high and the probability that the UAV has scatterers around is low [15]. Compared with the non-line-of-sight (NLOS) paths, the effect of LOS paths is determinant [19]. Therefore, we model the channel power gain from user  $k$  to the UAV as [8], [10]

$$h_k = \frac{\beta}{\|\mathbf{w}_0 - \mathbf{w}_k\|^2}, \quad k \in \mathcal{K} \quad (1)$$

where  $\beta$  denotes the reference channel gain at one meter away from user  $k$ .

For user  $k$ ,  $k \in \mathcal{K}$ , the computation task with  $R_k > 0$  computation input bits is partitioned into two parts with  $u_k \geq 0$  and  $v_k \geq 0$  bits. The former is offloaded to the UAV-enabled MEC server and the latter is computed locally. We assume that such a partition does not incur additional computation input bits, i.e.,  $R_k = u_k + v_k$  for  $k \in \mathcal{K}$ .

We focus on a particular time block with length  $T$ , which is not larger than the latency of MEC applications. During the time block  $T$ , we employ a TDMA protocol for all users to offload their computation tasks. Specifically, we divide the whole time block into  $K$  time slots, each with a length of  $\tau_k$ ,  $k \in \mathcal{K}$ . During the  $k$ th time slot, user  $k$  offloads its computation task, whose achievable offloading rate is

$$r_k = B \log_2 \left( 1 + \frac{p_k h_k}{\sigma^2} \right), \quad k \in \mathcal{K} \quad (2)$$

where  $B$  denotes the spectrum bandwidth,  $\sigma^2$  refers to the noise power at the UAV, and  $p_k$  refers to the transmit power of user  $k$ . Thus, the length of time slot allocated to user  $k$  for computation task offloading is

$$\tau_k = \frac{u_k}{r_k}, \quad k \in \mathcal{K}. \quad (3)$$

Substituting (3) into (2), the transmit power  $p_k$  is

$$p_k = \frac{\sigma^2}{h_k} \left( 2^{u_k / (B\tau_k)} - 1 \right). \quad (4)$$

For user  $k$ , besides the transmit power  $p_k$ , a constant circuit power  $q_k > 0$  is consumed [6]. The circuit power includes the power consumption from several circuit blocks in the transmission chain such as digital-to-analog converters, mixers, filters, frequency synthesizers, etc., which remains almost constant irrespective of the transmission rate [20], [21]. Therefore, the total offloading energy consumption at user  $k$  is

$$E_k = \tau_k(p_k + q_k). \quad (5)$$

In this paper, as in [6], we assume that the UAV-enabled MEC server has sufficient computation resources and consumes negligible computation time duration. Furthermore, the users are assumed to require negligible time duration to download the computed results.

*Remark 1:* For the MEC applications, we mean the applications such as face recognition [4], natural language processing [4], interactive gaming [4], [7], and object detection in video [7]. Take the face recognition as an example, if a mobile phone needs to identify whether a person is a legitimate user, it takes a photo and uploads it to the MEC server for the

face recognition. After the face recognition, the MEC server is required to feed back only one bit which indicates whether the person is a legitimate user. Thus, in the literature on MEC [4], [6], [7], negligible time duration to download the computed results is assumed.

*Remark 2:* In this paper, we mainly focus on the computing and communication offloading of users and thus negligible computation time duration at UAVs is assumed. However, in the real situation, the computation time duration is non-negligible. Thus, the queuing process of the computation tasks should be carefully considered [16], which is an interesting future work.

For computing task computed locally, we denote  $C_k$  as the number of central processing unit (CPU) cycles needed to calculate one input bit at user  $k$ . Employing dynamic voltage and frequency scaling (DVFS) techniques [1], user  $k$  can control the energy consumption for local computing by adjusting the CPU frequency, denoted as  $f_k$ . Since user  $k$  requires to finish local task computing within a block with length  $T$ , we have

$$f_k = \frac{C_k v_k}{T} = \frac{C_k (R_k - u_k)}{T}. \quad (6)$$

We apply a computing energy consumption model as in [2], [6], the energy required for user  $k$  to finish local task computing is expressed as

$$B_k = \zeta_k f_k^2 C_k v_k = \frac{\zeta_k C_k^3 (R_k - u_k)^3}{T^2} \quad (7)$$

where  $\zeta_k$  is the effective capacitance coefficient that depends on the chip architecture at user  $k$ .

Our goal in this paper is to minimize the system energy consumption of all users while ensuring the successful task computation of all users during a time block. To this end, we jointly optimize UAV position  $\mathbf{w}_0$ , time slot allocation  $\tau_k$ , as well as computation task partition  $u_k$  and  $v_k$  among different users. Thus, the formulated problem is

$$\begin{aligned} \min_{\mathbf{w}_0, \boldsymbol{\tau}, \mathbf{u}} \quad & \sum_{k=1}^K E_k + \sum_{k=1}^K B_k \\ \text{s.t.} \quad & \sum_{k=1}^K \tau_k \leq T, \quad \tau_k \geq 0, \quad 0 \leq u_k \leq R_k, \quad k \in \mathcal{K} \end{aligned} \quad (8)$$

where  $\boldsymbol{\tau} \triangleq [\tau_1, \dots, \tau_K]^T$  and  $\mathbf{u} \triangleq [u_1, \dots, u_K]^T$ . Because in the expression of  $E_k$ , the optimization variables  $\mathbf{w}_0$ ,  $\tau_k$ , and  $u_k$  are coupled, problem (8) is non-convex.

*Remark 3:* In this paper, the energy consumption of the UAV on both wireless communication and computation is not considered. The reason is explained as follows. The UAV-enabled MEC server is of high efficiency in disaster response, emergency relief or military scenarios [17]. In these applications, the limited energy supply and the lifetime of users are much more important than those of the UAV.

### III. JOINT OPTIMIZATION OF TIME SLOT ALLOCATION AND COMPUTATION TASK PARTITION GIVEN THE UAV POSITION

Given the UAV position, problem (8) is reduced to

$$\begin{aligned} \min_{\tau, u} \quad & \xi = \sum_{k=1}^K \frac{\tau_k}{h_k} g\left(\frac{u_k}{\tau_k}\right) + \sum_{k=1}^K \tau_k q_k + \sum_{k=1}^K \frac{\zeta_k C_k^3 (R_k - u_k)^3}{T^2} \\ \text{s.t.} \quad & \sum_{k=1}^K \tau_k \leq T, \quad \tau_k \geq 0, \quad 0 \leq u_k \leq R_k, \quad k \in \mathcal{K} \end{aligned} \quad (9)$$

where

$$g(x) \triangleq \sigma^2 \left[ \exp\left(\frac{x \ln 2}{B}\right) - 1 \right]. \quad (10)$$

Since  $g(x)$  is a convex function, the perspective of  $g(x)$ ,  $(\tau_k/h_k)g(u_k/\tau_k)$ , is a convex function with respect to  $\tau_k$  and  $u_k$ . Thus, problem (9) is a convex optimization problem.

In the following, we will employ augmented Lagrangian active set method to obtain the low-complexity solution to problem (9). Omitting the soft constraints of problem (9), we have the following unconstraint optimization problem

$$\min_{\tau, u} \xi. \quad (11)$$

Taking the first-order partial derivative of the objective function of problem (11)  $\xi$  with respect to  $\tau_k$ , from Karush-Kuhn-Tucker (KKT) conditions, we have

$$\frac{\partial \xi}{\partial \tau_k} = \frac{1}{h_k} \left[ g\left(\frac{u_k}{\tau_k}\right) - \frac{u_k}{\tau_k} g'\left(\frac{u_k}{\tau_k}\right) \right] + q_k = 0 \quad (12)$$

where

$$g'(x) = \frac{\sigma^2 \ln 2}{B} \exp\left(\frac{x \ln 2}{B}\right) \quad (13)$$

is the first-order derivative of  $g(x)$  with respect to  $x$ . For the function

$$y = g(x) - x g'(x) \quad (14)$$

with  $x > 0$ , its inverse function is shown to be

$$x = \frac{B}{\ln 2} \left( \mathcal{W}\left(-\frac{y}{\sigma^2 e} - \frac{1}{e}\right) + 1 \right) \quad (15)$$

where  $\mathcal{W}(x)$  refers to the principal branch of the Lambert  $\mathcal{W}$  function, defined as the solution for  $\mathcal{W}(x)e^{\mathcal{W}(x)} = x$ , and  $e$  refers to the base of the natural logarithm. Let

$$\theta_k = \frac{u_k}{\tau_k}. \quad (16)$$

From (15), we know that the optimal  $\theta_k$  of the unconstraint optimization problem  $\min_{\theta, u} \xi$  is

$$\theta_k^* = \frac{B}{\ln 2} \left( \mathcal{W}\left(\frac{q_k h_k}{\sigma^2 e} - \frac{1}{e}\right) + 1 \right) \quad (17)$$

where  $\theta \triangleq [\theta_1, \dots, \theta_K]^T$ . Taking the first-order partial derivative of  $\xi$  with respect to  $u_k$ , from KKT conditions, we have

$$\frac{\partial \xi}{\partial \tau_k} = \frac{1}{h_k} g'\left(\frac{u_k}{\tau_k}\right) - \frac{3\zeta_k C_k^3 (R_k - u_k)^2}{T^2} = 0. \quad (18)$$

Substituting (13) into (18), after some mathematical manipu-

lations, we have

$$u_k^* = \left[ R_k - \sqrt{\frac{T^2 \sigma^2 2^{(\theta_k^*/B)} \ln 2}{3\zeta_k C_k^3 B h_k}} \right]^+ \quad (19)$$

where  $[x]^+$  refers to  $\max\{x, 0\}$ . Obtaining  $\theta_k^*$  and  $u_k^*$ , we can obtain  $\tau_k^*$  using (16).

From the augmented Lagrangian active set method, by noting that  $0 \leq u_k^* \leq R_k$ , the optimal value of  $u_k$  to problem (9) is  $u_k^o = u_k^*$ .

From (17) and properties of the Lambert  $\mathcal{W}$  function, since  $\frac{q_k h_k}{\sigma^2 e} > 0$ , we have  $\theta_k^* > 0$ . Thus,  $\tau_k^* \geq 0$ . If  $\sum_{k=1}^K \tau_k^* \leq T$ , all of the soft constraints in problem (9) are satisfied. The optimal value of  $\tau_k$  to problem (9) is  $\tau_k^o = \tau_k^*$ .

If  $\sum_{k=1}^K \tau_k^* > T$ , from the augmented Lagrangian active set method, the constraint  $\sum_{k=1}^K \tau_k \leq T$  in problem (9) is active, i.e.,  $\sum_{k=1}^K \tau_k = T$ . We should solve the following unconstraint optimization problem

$$\min_{\tau, u} \xi + \mu \left( \sum_{k=1}^K \tau_k - T \right) \quad (20)$$

where  $\mu > 0$  denotes the Lagrangian dual variable associated with the constraint  $\sum_{k=1}^K \tau_k = T$ .

Using the similar steps as the solution to problem (11), we know that the optimal  $\theta_k$  of problem (20) is

$$\tilde{\theta}_k(\mu) = \frac{B}{\ln 2} \left( \mathcal{W}\left(\frac{(q_k + \mu) h_k}{\sigma^2 e} - \frac{1}{e}\right) + 1 \right) \quad (21)$$

and the optimal  $u_k$  of problem (20) is

$$\tilde{u}_k(\mu) = \left[ R_k - \sqrt{\frac{T^2 \sigma^2 2^{(\tilde{\theta}_k(\mu)/B)} \ln 2}{3\zeta_k C_k^3 B h_k}} \right]^+. \quad (22)$$

Obtaining  $\tilde{\theta}_k(\mu)$  and  $\tilde{u}_k(\mu)$ , we can obtain  $\tilde{\tau}_k(\mu)$  using (16).

In (21) and (22), there still exists an unknown variable  $\mu$ . The value of  $\mu$  is determined by the equation  $\sum_{k=1}^K \tilde{\tau}_k(\mu) = T$ . Since the expression of  $\tilde{\tau}_k(\mu)$  is complicated, the aforementioned equation is difficult to solve. Instead of one-dimensional search over possible value of  $\mu$  to solve equation  $\sum_{k=1}^K \tilde{\tau}_k(\mu) = T$ , we propose a bisection search method in this paper.

To proceed, we have the following lemma.

**Lemma 1:**  $\tau_k(\mu)$  is a monotonically decreasing function (MDF) of  $\mu$ .

*Proof:* Since  $\mu > 0$ , we have  $\frac{(q_k + \mu) h_k}{\sigma^2 e} - \frac{1}{e} > -\frac{1}{e}$ . Because  $\mathcal{W}(x)$  is a monotonically increasing function (MIF) of  $x \geq -\frac{1}{e}$ . Thus,  $\tilde{\theta}_k(\mu)$  is an MIF of  $\mu$  and  $\tilde{u}_k(\mu)$  is an MDF of  $\mu$ . Accordingly,  $\tau_k(\mu)$  is an MDF of  $\mu$ . ■

From Lemma 1, the bisection search method can be employed to solve the equation  $\sum_{k=1}^K \tilde{\tau}_k(\mu) = T$ . In the following, we derive the bisection search upper and lower bounds on  $\mu$ . Since  $\mu > 0$ , the lower bound (LB) on  $\mu$  is  $\mu_{LB} = 0$ .

The upper bound (UB) on  $\mu$  is derived as follows. From

(22),  $\tilde{u}_k(\mu)$  is lower bounded by 0. Thus, we have

$$R_k \geq \sqrt{\frac{T^2 \sigma^2 2^{(\tilde{\theta}_k(\mu)/B)} \ln 2}{3\zeta_k C_k^3 B h_k}}. \quad (23)$$

Substituting (21) into (23), after some mathematical manipulation, we obtain

$$\mathcal{W}\left(\frac{(q_k + \mu)h_k}{\sigma^2 e} - \frac{1}{e}\right) \leq \varphi_k - 1 \quad (24)$$

where

$$\varphi_k = \ln \frac{3\zeta_k C_k^3 B h_k R_k^2}{T^2 \sigma^2 \ln 2}. \quad (25)$$

From the definition of Lambert  $\mathcal{W}$  function, the UB on  $\mu$  is

$$\mu_{\text{UB}} = \min_k \frac{(\varphi_k - 1)e^{\varphi_k} \sigma^2 + \sigma^2}{h_k} - q_k. \quad (26)$$

Obtaining the solution to the equation  $\sum_{k=1}^K \tilde{\tau}_k(\mu) = T$ , denoted as  $\tilde{\mu}$ , we can obtain  $\tilde{u}_k(\tilde{\mu})$  and  $\tilde{\tau}_k(\tilde{\mu})$ .

From the augmented Lagrangian active set method, by noting that  $0 \leq \tilde{u}_k(\tilde{\mu}) \leq R_k$ , the optimal value of  $u_k$  to problem (9) is  $u_k^o = \tilde{u}_k(\tilde{\mu})$ . Furthermore, since  $\tilde{\tau}_k(\tilde{\mu}) \geq 0$  and  $\sum_{k=1}^K \tilde{\tau}_k(\tilde{\mu}) = T$ , all of the soft constraints in problem (9) are satisfied. The optimal value of  $\tau_k$  to problem (9) is  $\tau_k^o = \tilde{\tau}_k(\tilde{\mu})$ .

Obtaining the solution to problem (9), the globally optimal solution to problem (8) can be found by 2D search over  $x_0$  and  $y_0$  where in each iteration, problem (9) is solved. To reduce the computational complexity, we can employ alternating optimization to find the locally optimal solution to problem (8). Employing alternating optimization, we should optimize the UAV position, i.e.,  $x_0$  and  $y_0$ , given the time slot allocation,  $\tau$ , and the computation task partition,  $\mathbf{u}$ .

#### IV. OPTIMIZATION OF UAV POSITION GIVEN THE TIME SLOT ALLOCATION AND THE COMPUTATION TASK PARTITION

Given the time slot allocation and the computation task partition, problem (8) is reduced to

$$\min_{\mathbf{w}_0} \sum_{k=1}^K \frac{\sigma^2 \tau_k \rho_k}{h_k} \quad (27)$$

where  $\rho_k = 2^{u_k/(B\tau_k)} - 1$ . Substituting (1) into (27), we have

$$\min_{x_0, y_0} \phi = \sum_{k=1}^K \sigma^2 \beta^{-1} \tau_k \rho_k \left[ (x_0 - x_k)^2 + (y_0 - y_k)^2 + H^2 \right]. \quad (28)$$

Problem (28) is a convex optimization problem. Taking the first-order partial derivatives of  $\phi$  with respect to  $x_0$  and  $y_0$ , respectively, and apply KKT conditions, we obtain

$$\frac{\partial \phi}{\partial x_0} = \sum_{k=1}^K 2\sigma^2 \beta^{-1} \tau_k \rho_k (x_0 - x_k) = 0, \quad (29)$$

$$\frac{\partial \phi}{\partial y_0} = \sum_{k=1}^K 2\sigma^2 \beta^{-1} \tau_k \rho_k (y_0 - y_k) = 0. \quad (30)$$

Thus, the closed-form solution to problem (28) is

$$x_0^o = \frac{\sum_{k=1}^K 2\sigma^2 \beta^{-1} \tau_k \rho_k x_k}{\sum_{k=1}^K 2\sigma^2 \beta^{-1} \tau_k \rho_k}, \quad (31)$$

$$y_0^o = \frac{\sum_{k=1}^K 2\sigma^2 \beta^{-1} \tau_k \rho_k y_k}{\sum_{k=1}^K 2\sigma^2 \beta^{-1} \tau_k \rho_k}. \quad (32)$$

*Remark 4:* It is noted that problem (8) is non-convex because in the expression of  $E_k$ , the optimization variables  $\mathbf{w}_0$ ,  $\tau$ , and  $\mathbf{u}$  are coupled. We propose to employ alternating optimization to iteratively optimize  $(\tau, \mathbf{u})$  and  $\mathbf{w}_0$ . For the optimization of  $(\tau, \mathbf{u})$ , i.e., problem (11), we obtain the globally optimal solution. For the optimization of  $\mathbf{w}_0$ , i.e., problem (27), we also obtain the globally optimal solution. However, since the alternating optimization is employed, we only obtain the locally optimal solution to problem (8).

*Complexity Analysis:* For our proposed alternating optimization scheme, the computational complexity is mainly on the bisection search of  $\mu$  to solve equation  $\sum_{i=1}^K \tilde{\tau}_k(\mu) = T$ . The computational complexity of the bisection search is  $\mathcal{O}(\log_2(\epsilon^{-1}(\mu_{\text{UB}} - \mu_{\text{LB}})))$ , where  $\epsilon$  denotes the bisection search accuracy. Thus, the computational complexity of our proposed alternating optimization scheme is

$$\mathcal{O}(L_1 \cdot \log_2(\epsilon^{-1}(\mu_{\text{UB}} - \mu_{\text{LB}}))) \quad (33)$$

$\mathcal{O}(L_1 \cdot \log_2(\epsilon^{-1}(\mu_{\text{UB}} - \mu_{\text{LB}})))$ , where  $L_1$  denotes the average number of iterations for the convergence of alternating optimization.

For our proposed 2D search scheme, the computational complexity is

$$\mathcal{O}\left(\frac{x_{\max} - x_{\min}}{\epsilon_x} \cdot \frac{y_{\max} - y_{\min}}{\epsilon_y} \log_2 \frac{\mu_{\text{UB}} - \mu_{\text{LB}}}{\epsilon}\right) \quad (34)$$

where  $x_{\max} = \max\{x_k, k \in \mathcal{K}\}$ ,  $x_{\min} = \min\{x_k, k \in \mathcal{K}\}$ ,  $y_{\max} = \max\{y_k, k \in \mathcal{K}\}$  and  $y_{\min} = \min\{y_k, k \in \mathcal{K}\}$ ,  $\epsilon_x$  and  $\epsilon_y$  denote the 2D search accuracies over  $x$ -axis and  $y$ -axis, respectively.

*Scalability:* From (33) and (34), the computational complexities of our proposed alternating optimization scheme and 2D search scheme are not related with the number of users,  $K$ . With the increase of  $K$ , the computational complexities remain the same.

#### V. NUMERICAL RESULTS

In simulations, we assume that the UAV is flying at  $H = 10$  meters. The number of users on the ground is  $K = 8$ . The locations of users are uniformly distributed in a  $100 \times 100$  m<sup>2</sup> square area. For computation task offloading, the constant circuit power consumed at each user is  $q_1 = q_2 = \dots = q_8 = 10^{-4}$  W [6]. The computation input bits of the computation task at users are  $R_1 = R_2 = \dots = R_7 = R/2$  bits and  $R_8 = 4R$  bits. The spectrum bandwidth for offloading is  $B = 2$  MHz. The number of CPU cycles needed to calculate one input bit at users are  $C_1 = C_2 = \dots = C_8 = 10^3$  cycles/bit [6]. The effective capacitance coefficients are  $\zeta_1 = \zeta_2 = \dots = \zeta_8 = 10^{-28}$  [6]. The noise power at the UAV is  $\sigma^2 = 10^{-9}$  W. The reference channel gain at one meter away from each user is  $\beta = 30$  dB [8], [10].

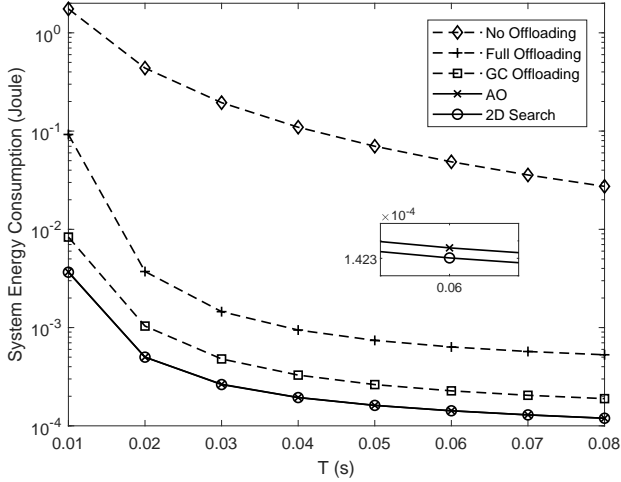


Fig. 1. System energy consumption versus the time block length  $T$ ; performance comparison of different schemes when  $R = 3 \times 10^4$  bits.

In Fig. 1, we present the system energy consumption comparison for different schemes when  $R = 3 \times 10^4$  bits and the time block length  $T$  is from 0.01 s to 0.08 s. In the legend, “AO” and “2D Search” refer to our proposed alternating optimization scheme and 2D search scheme, respectively. “No Offloading” refers to that the users conduct computation tasks only locally without offloading. “Full Offloading” refers to that the users offload all computation tasks to the UAV-enabled MEC server. “GC Offloading” refers to that only joint optimization of time slot allocation and computation task partition is considered without UAV position optimization, where the UAV is flying over the gravity center of users, i.e., we solve problem (11) using the method proposed in Section III given that  $w_0$  is over the gravity center of users. From Fig. 1, it is observed that the system energy consumption obtained by our proposed alternating optimization scheme matches to that obtained by the 2D search scheme. Furthermore, our proposed schemes outperform the “No Offloading”, “Full Offloading”, and “GC Offloading” schemes. The reason is explained as follows. The obtained values of  $w_0$ ,  $\tau$ , and  $u$  by the “No Offloading”, “Full Offloading”, and “GC Offloading” schemes are all feasible to problem (8). Since in aforementioned schemes,  $w_0$ ,  $\tau$ , and  $u$  are not jointly optimized, the achieved objective values of problem (8) are worse than those achieved by our proposed jointly optimization schemes.

*Remark 5:* In (1), the path loss factor is 2. The path loss factor which is larger than 2 may result in the performance mismatch between our proposed alternating optimization scheme and the 2D search scheme.

*Remark 6:* From Fig. 1, it is found that the system energy consumptions of all schemes decrease with the increase of  $T$ . This is because for problem (8),  $\sum_{k=1}^K \tau_k \leq T$  is a constraint. Larger  $T$  means looser constraint. Thus, with the increase of  $T$ , the smaller objective value can be achieved.

In Fig. 2, we present the system energy consumption comparison for different schemes when  $T = 0.08$  s and  $R$  is from  $3 \times 10^4$  bits to  $10^5$  bits. From Fig. 2, it is illustrated

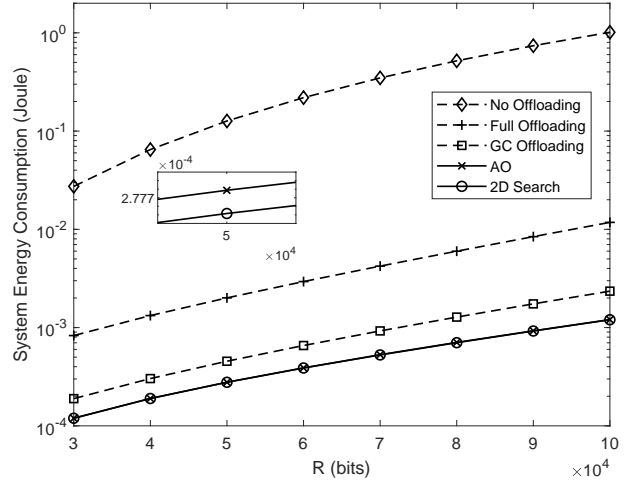


Fig. 2. System energy consumption versus  $R$ ; performance comparison of different schemes when  $T = 0.08$  s.

that our proposed schemes are superior to the “No Offloading”, “Full Offloading”, and “GC Offloading” schemes.

## VI. CONCLUSION

In this paper, we have derived the globally and locally optimal solutions to the joint optimization problem for a multiuser aerial MEC system. Numerical results demonstrate that our proposed schemes are superior to the no offloading, full offloading, and gravity center offloading schemes.

## REFERENCES

- [1] Y. Mao, C. You, J. Zhang, K. Huang, and K. B. Letaief, “A survey on mobile edge computing: The communication perspective,” *IEEE Commun. Survey Tuts.*, vol. 19, no. 4, pp. 2322-2358, 4th Quart., 2017.
- [2] D. Huang, P. Wang, and D. Niyato, “A dynamic offloading algorithm for mobile computing,” *IEEE Trans. Wireless Commun.*, vol. 11, no. 6, pp. 1991-1995, Jun. 2012.
- [3] Y. Wang, M. Sheng, X. Wang, L. Wang, and J. Li, “Mobile edge computing: Partial computation offloading using dynamic voltage scaling,” *IEEE Trans. Commun.*, vol. 64, no. 10, pp. 4268-4282, Aug. 2016.
- [4] X. Chen, “Decentralized computation offloading game for mobile cloud computing,” *IEEE Trans. Parallel and Distrib. Syst.*, vol. 26, no. 4, pp. 974-983, Apr. 2015.
- [5] X. Chen, L. Jiao, W. Li, and X. Fu, “Efficient multi-user computation offloading for mobile-edge cloud computing,” *IEEE/ACM Trans. Netw.*, vol. 24, no. 5, pp. 2795-2808, Oct. 2016.
- [6] F. Wang, J. Xu, X. Wang, and S. Cui, “Joint offloading and computing optimization in wireless powered mobile-edge computing systems,” *IEEE Trans. Wireless Commun.*, vol. 17, no. 3, pp. 1784-1797, Mar. 2018.
- [7] C. You, Y. Zeng, R. Zhang, and K. Huang, “Asynchronous mobile-edge computation offloading: Energy-efficient resource management,” *IEEE Trans. Wireless Commun.*, vol. 17, no. 11, pp. 7590-7605, Nov. 2018.
- [8] Y. Zeng, R. Zhang, and T. J. Lim, “Wireless communications with unmanned aerial vehicles: Opportunities and challenges,” *IEEE Commun. Mag.*, vol. 54, no. 5, pp. 36-42, May 2016.
- [9] E. Bertran and A. Sánchez-Cerdà, “On the tradeoff between electrical power consumption and flight performance in fixed-wing UAV autopiots,” *IEEE Trans. Veh. Technol.*, vol. 56, no. 11, pp. 8832-8840, Nov. 2016.
- [10] M. Cui, G. Zhang, Q. Wu, and D. W. K. Ng, “Robust trajectory and transmit power design for secure UAV communications,” *IEEE Trans. Veh. Technol.*, vol. 67, no. 9, pp. 9042-9046, Sept. 2018.
- [11] D. Yang, Q. Wu, Y. Zeng, and R. Zhang, “Energy tradeoff in ground-to-UAV communication via trajectory design,” *IEEE Trans. Veh. Technol.*, vol. 67, no. 7, pp. 6721-6726, Jul. 2018.

- [12] F. Cheng, S. Zhang, Z. Li, Y. Chen, N. Zhao, F. R. Yu, and V. C. M. Leung, "UAV trajectory optimization for data offloading at the edge of multiple cells," *IEEE Trans. Veh. Technol.*, vol. 67, no. 7, pp. 6732-6736, Jul. 2018.
- [13] Y. Takahashi, Y. Kawamoto, H. Nishiyama, N. Kato, F. Ono, and R. Miura, "A novel radio resource optimization method for relay-based unmanned aerial vehicles," *IEEE Trans. Wireless Commun.*, vol. 17, no. 11, pp. 7352-7363, Nov. 2018.
- [14] F. Tang, Z. M. Fadlullah, N. Kato, F. Ono, and R. Miura, "AC-POCA: Anticoordination game based partially overlapping channels assignment in combined UAV and D2D-based networks," *IEEE Trans. Veh. Technol.*, vol. 67, no. 2, pp. 1672-1683, Feb. 2018.
- [15] N. Rupasinghe, Y. Yapici, I. Güvenc, and Y. Kakishima, "Non-orthogonal multiple access for mmWave drone networks with limited feedback," *IEEE Trans. Commun.*, vol. 67, no. 1, pp. 762-777, Jan. 2019.
- [16] F. Tang, Z. M. Fadlullah, B. Mao, N. Kato, F. Ono, and Ryu Miura, "On a novel adaptive UAV-mounted cloudlet-aided recommendation system for LBSNs," *IEEE Trans. Emerging Topics in Computing*, to be published.
- [17] S. Jeong, O. Simeone, and J. Kang, "Mobile edge computing via a UAV mounted cloudlet: Optimization of bit allocation and path planning," *IEEE Trans. Veh. Technol.* vol. 67, no. 3, pp. 2049-2063, Mar. 2018.
- [18] F. Zhou, Y. Wu, H. Sun, and Z. Chu, "UAV-enabled mobile edge computing: Offloading optimization and trajectory design," in *Proc. ICC 2018*, pp. 1-6.
- [19] Z. Ding, P. Fan, and H. V. Poor, "Random beamforming in millimeter-wave NOMA networks," *IEEE Access*, vol. 5, pp. 7667-7681, Jun. 2017.
- [20] H. Kim and G. de Veciana, "Leveraging dynamic spare capacity in wireless systems to conserve mobile terminals' energy," *IEEE/ACM Trans. Netw.*, vol. 18, no. 3, pp. 802-815, Jun. 2010.
- [21] Q. Wu, M. Tao, and W. Chen, "Joint Tx/Rx energy-efficient scheduling in multi-radio wireless networks: A divide-and-conquer approach," *IEEE Trans. Wireless Commun.*, vol. 15, no. 4, pp. 2727-2740, Apr. 2016.